



Published in final edited form as:

Sens Actuators B Chem. 2007 January 30; 121(1): 36–46.

Improving Blood Compatibility of Intravascular Oxygen Sensors Via Catalytic Decomposition of S-Nitrosothiols to Generate Nitric Oxide *In Situ*

Yiduo Wu¹, Alvaro P. Rojas², Grant W. Griffith², Amy M. Skrzypchak², Nathan Lafayette², Robert H. Bartlett², and Mark E. Meyerhoff^{1,*}

¹ Department of Chemistry, University of Michigan

² Department of General Surgery, University of Michigan

Abstract

Reliable, real-time, *in vivo* sensing (intravascular) of blood gases and electrolytes remains a difficult challenge owing to biocompatibility issues that occur when chemical sensors are implanted into the blood stream. Recently, local release of nitric oxide (NO) at the sensor/blood interface has been suggested as a potential solution to this problem. However, the lifetime of NO release from thin polymer films coated on implanted sensors is limited by the reservoir of NO donor loaded within the polymeric coating. To continuously produce NO at the sensor/blood interface, a novel approach to catalytically decompose endogenous S-nitrosothiols (RSNOs) in blood to generate NO *in situ* is reported herein. Metallic copper particles of two different sizes (3 μm and 80 nm) are embedded as catalysts in thin polymer coatings on the surface intravascular electrochemical oxygen sensing catheters. Oxygen levels (partial pressure of oxygen; PO_2) provided by the copper particle/polymer coated sensors are, on average, more accurate than values obtained from non-NO generating control sensors when both types of sensors are implanted in porcine arteries for 19–20 h. Upon termination of each *in vivo* study, catheters were explanted and examined for surface thrombosis via both visual image and lactate dehydrogenase (LDH) assay. The results indicate that the Cu^0 -catalyst coatings significantly reduce the occurrence of surface thrombosis, likely from the ability to generate NO from endogenous RSNO species at the sensor/blood interface.

Keywords

nitric oxide generation; S-nitrosothiols; copper catalyst; intravascular electrochemical oxygen sensor

1. Introduction

Monitoring the cardiopulmonary function of critically ill patients mandates the continuous measurements of blood gases and electrolytes. The development of implantable sensors (electrochemical and/or optical) capable of reliably measuring important physiological species, such as PO_2 , PCO_2 , pH, electrolytes, glucose and lactate *in vivo*, has remained a great challenge for several decades [1,2]. A variety of prototype catheter-style commercial devices have been

* To whom correspondence should be addressed at: 930 N. University Ave., University of Michigan, Ann Arbor, MI 48109-1055. E-mail: mmeyerho@umich.edu. Tel: 734-763-5916. Fax: 734-647-4865..

Publisher's Disclaimer: This is a PDF file of an unedited manuscript that has been accepted for publication. As a service to our customers we are providing this early version of the manuscript. The manuscript will undergo copyediting, typesetting, and review of the resulting proof before it is published in its final citable form. Please note that during the production process errors may be discovered which could affect the content, and all legal disclaimers that apply to the journal pertain.

developed for intravascular blood gas sensing purposes [3,4]. However, these devices have not found widespread use in the clinical arena, primarily due to the erratic results obtained when used for continuous *in vivo* measurements. Such errant results arise from the biological responses of living systems to foreign devices implanted in the blood stream. Proteins, such as collagen, fibrinogen and von Willebrand factor, adsorb onto the polymer surfaces of the implanted sensors within seconds [5,6]. The adsorbed protein layer mediates the adhesion and activation of metabolically active cells, e.g., platelets, that later arrive [7,8]. Platelets play a key role in blood coagulation since activated platelets keep recruiting circulating cells to the polymer surfaces which ultimately leads to the formation of blood clots [9]. The presence of active cells on the surface of such devices causes a localized change in pH, PO_2 and PCO_2 values due to cellular respiration compared to the bulk blood [1], yielding significant errors when results are compared to values obtained from *in vitro* measurements on discrete samples of blood.

Nitric oxide has been widely recognized as a potent vasodilator and inhibitor of platelet adhesion and activation [10–13]. It is produced from L-arginine by a class of enzymes known as nitric oxide synthases (NOS). The perfect thromboresistance of the human endothelium has been partly attributed to the low but continuous production of NO in this layer [14,15]. Endothelial cells that line the inner walls of healthy blood vessels produce NO with an estimated surface flux level of $0.5 - 4.0 \times 10^{-10} \text{ mol cm}^{-2} \text{ min}^{-1}$ [16]. Therefore, one approach to potentially resolve the hemocompatibility problem is to release or generate NO locally at the blood/sensor interface at or above the flux from normal endothelial cells in order to inhibit platelet adhesion and activation, and thus prevent gross thrombus formation. Biomedical devices (i.e., intravascular sensors, vascular grafts, extracorporeal circuits, etc.) coated with polymers containing diazeniumdiolate-type NO donors have already been shown to exhibit improved biocompatibility via various *in vivo* evaluations (in animal models) [17–19]. However, due to the limited reservoir of the NO donors in the polymer coatings, the NO-release approach is only suitable for biomedical devices that require short-term blood contact times, such as hemodialysis and extracorporeal circulation, but not for long-term (i.e., weeks or months) implantation. To maintain NO production for extended periods of time it may be possible to take advantage of endogenous species such as nitrosothiols (RSNOs) that are constantly produced in the body (from NO generated by NOS) to generate NO *in situ* at the polymer/blood interface.

Nitric oxide has very short lifetime in blood [20] due to its reactivity with various blood components [21]. In contrast, a more abundant (i.e., micromolar concentrations) and stable form of NO in blood are *S*-nitroso adducts with thiol groups (RSNOs) [22], such as *S*-nitrosoalbumin (AlbSNO), *S*-nitrosocysteine (CysNO) and *S*-nitrosogluthathione (GSNO) [22–24]. One well-known mechanism of RSNO decomposition to yield NO is catalyzed by Cu^+ [25], in which Cu^+ is produced from the reduction of Cu^{2+} by thiolates or other reducing equivalents that exist in the physiological environment (e.g., ascorbate). We have already demonstrated that polymer films doped with lipophilic cyclen-type Cu(II) complexes [26] and Cu(II)-cyclen complex covalently linked to poly(2-hydroxyethyl methacrylate) hydrogels [27] are capable of generating significant NO fluxes ($>1 \times 10^{-10} \text{ mol cm}^{-2} \text{ min}^{-1}$) in the presence of physiologically relevant concentrations of GSNO and appropriate reducing agents. However, our preliminary studies indicate that such polymer films based on these Cu(II)-cyclen complexes are not ideally suited for long-term NO-generation *in vivo* due to the loss of NO-generating functionality after extended storage in plasma. In this paper, we report the use of polymer films doped with small metallic copper particles as the catalytic coatings on the surface of intravascular electrochemical oxygen sensing catheters. Such coatings can generate NO *in situ* at the sensor/blood interface via a slow corrosion of the copper particles to produce copper ions. When placed in porcine arteries, the oxygen sensing catheters with NO-generating capability are shown to exhibit improved blood compatibility and more accurate PO_2

measurements when compared to corresponding control oxygen sensing catheters implanted within the same animals.

2. Experimental Section

2.1. Materials

Sodium chloride, potassium chloride, sodium nitrite, reduced L-glutathione (GSH), sulfuric acid (95–98%), bichinchonic acid (disodium salt), dibutyltin dilaurate (95%), Triton X-100, bovine serum albumin and 3- μm copper powder were purchased from Sigma-Aldrich (St. Louis, MO). Copper nanoparticles (80 nm size) were from Inframat Advanced Materials (Farmington, CT). Ethylenediaminetetraacetic acid (EDTA) was obtained from Mallinckrodt (Paris, KY). Methocel 90 HG and 3-aminopropyltrimethoxy-silane were from Fluka (Milwaukee, WI). The silicone rubber tubing (0.51 mm i.d. \times 0.94 mm o.d.) used to construct catheters was obtained from Helix Medical, Inc. (Carpinteria, CA), and Silastic medical grade tubing (0.94 mm i.d. \times 1.29 mm o.d.) was received as a gift from Medtronic (Minneapolis, MN). Silicone rubber (RTV-3140) was the product of Dow Corning (Midland, MI). Tecophilic SP-60D-60 and Tecoflex SG-80A polyurethanes were from Noveon (Cleveland, OH). A quick-setting two-part epoxy was the product of Super Glue Corp. (Rancho Cucamonga, CA). The PTFE-coated Pt/Ir and Ag wires employed to fabricate the oxygen sensing catheters were products of MedwireCorp. (Mt. Vernon, NY). Ultra 4-way stopcocks and Angiocath catheter guides (16g \times 1.16 in) used for catheter implantation in the arteries of pigs were from Medex (Hillard, OH) and Becton Dickinson (Sandy, UT), respectively.

2.2. Fabrication of NO-generating oxygen sensors

The Clark-type amperometric oxygen sensing catheters employed in this work were fabricated as previously reported [17,19]. However, instead of applying an NO-release polymer coating on the surface of the silicone rubber catheter, a thin layer of a polymer doped with Cu^0 catalyst (in the form of either micron- or nano-sized Cu^0 particles) was coated on the surface of the silicone rubber tubing (see Figure 1). Briefly, the sensor sleeves were made by cutting the thinner silicone rubber tubing (from Helix Medical) into 25 mm pieces and filling \sim 2 mm length on one end with RTV-3140. The sensor sleeves were cured under ambient conditions for 24 h. Two different sizes of copper particles (3 μm and 80 nm) were evaluated for *in vivo* biocompatibility, together with their respective controls (polymer coating without Cu^0 particles). In the case of 3- μm Cu^0 particle coatings, 3% (w/v) of Cu^0 particles were suspended in a THF solution of 5% (w/v) RTV-3140 and 2.5% (w/v) SP-60D-60 hydrophilic polyurethane (HPPU). This mixture was sonicated for 30 min before the catheter sleeves were dip-coated once in this suspension. Thirty minutes later, one top-coat of 1% RTV-3140 and 0.5% HPPU (w/v) was applied to the sensor sleeves by dip-coating. The coatings were first cured overnight at ambient moisture, and then further dried under vacuum for 24 h. Coatings on control sensors were prepared in the same manner except that no copper particles were added to the polymer solution used for the underlying coating.

To apply the polymer coating doped with the copper nanoparticles to the sensors, an adhesion promoting layer was added between the silicone rubber sensor sleeve and the Tecoflex SG-80A polyurethane layer which contained the copper nanoparticles. This adhesion layer was made from 10% RTV-3140, 1% 3-aminopropyltrimethoxy-silane and 0.1% dibutyltin dilaurate catalyst (all w/v) in THF. This adhesion layer was cured under ambient moisture for 24 h before the catalyst layer was dip-coated on the sensor. The catalytic layer was prepared using a THF solution with 3 w/v% of Tecoflex SG-80A and 1 w/v% Cu^0 nanoparticle catalyst and sonicated for 20 min. The sensor sleeves with the adhesion promoter layer were dip-coated once in this polymer mixture and dried under ambient conditions overnight and then dried again under vacuum for 24 h. Control sensor sleeves were coated in the same manner with the only

difference being the absence of copper particles in the outer polymer layer. No additional topcoat was applied to prepare the sensors with the nanoparticle-based coating.

To construct the functional electrochemical oxygen-sensing catheter, the sensor sleeves were filled with 0.15 M KCl and 1.5 wt% Methocel internal electrolyte solution (see Figure 1). The entire sensor sleeve was sealed and glued to the sensor body by epoxy. The Teflon coated Pt/Ir working electrode was polarized at -0.7 V vs. the Ag/AgCl reference electrode. Current output was recorded via a DATAQ Instruments DA-700 USB data acquisition card (Akron, OH) by WinDAQ/Lite software. The sensor's response to oxygen was evaluated via bench experiments by using different tonometered solutions of oxygen (0, 5, 10, 21 and 30% of O₂, balanced with N₂). Sensors were placed in each solution for 10 min and the output current was recorded by the aforementioned protocol.

2.3. Nitric oxide generation in vitro

The NO-generating ability of sensor sleeves was examined before and after the *in vivo* studies using a chemiluminescence NO analyzer. Nitrosoglutathione (GSNO) was prepared by the reaction of equal-molar glutathione (GSH) and NaNO₂ in 0.06 M H₂SO₄. To an amber glass reaction cell containing 2 mL PBS (138 mM NaCl, 2.7 mM KCl and 10 mM sodium phosphate, pH 7.4) was added 1 μ M GSNO, 30 μ M GSH and 5 μ M EDTA (to chelate metal ion contaminants that might otherwise decompose GSNO). The solution was bathed at 37°C and continuously bubbled with N₂. Any NO produced in the test solution was purged from the buffer, carried by the N₂ gas into the chemiluminescence reaction chamber and monitored in real-time. The baseline NO level was recorded for ~ 5 min before the Cu⁰-containing sensor sleeves were placed in the substrate solution.

2.4. In vitro copper corrosion

The copper-containing sensor sleeves were bathed in 5 mL PBS (pH 7.4) for 1 d at 37°C under constant shaking. The bathing solution was then tested for copper content using a bicinchoninic acid (BCA) assay as previously reported [28]. The calibration standards were prepared via serial dilution from a stock 1000 ppm Cu(NO₃)₂ (Fisher) solution into PBS. The absorbance at 357 nm was used for quantification.

2.5. In vivo evaluation

Assessment of the *in vivo* biocompatibility and analytical performance of the NO-generating oxygen sensing catheters was performed by implanting sensors in nine female juvenile swine, weighing 25 – 30 kg. Six of the nine animals were used for the evaluation of the 3- μ m Cu⁰ particle based coating and the remaining three animals were used to assess the sensors with polymer coatings containing the Cu⁰ nanoparticles. Mechanical gas anesthesia was maintained during the experiment with a mix of 1–3% liquid for inhalation isoflurane (Hospira, Inc., Lake Forest, IL) and 21% oxygen. The depth of anesthesia was monitored following the University of Michigan's University Committee on Use and Care of Animals protocol that was pre-approved for these experiments.

Cut-downs of the animals were made on both groins as well as the bilateral sides of the neck for isolation of the femoral and carotid arteries, respectively. An arterial 14-gauge catheter was advanced into the right thyrocervical trunk to monitor systemic hemodynamics (blood pressure and heart rate) and to acquire blood samples for activated coagulation time (ACT) and *in vitro* arterial blood gas (ABG) values using a Radiometer Medical ABL-505 standard blood gas analyzer (Copenhagen, Denmark). The right internal jugular vein was exposed and dissected from surrounding tissues and a 9 Fr Arrow® catheter was advanced to monitor central venous pressure (CVP), and to further administer i.v. fluids (lactated ringers) and medications. The arterial and CVP lines were attached to fluid pressure transducers (Abbot Critical Care

Systems, North Chicago, IL) and monitored continuously on a Series 7000 Pressure Monitor (Marquette Electronics, Milwaukee, WI). The bladder of each animal was surgically drained by placing a Foley catheter directly into the bladder.

For each swine, four sensors were implanted: two NO-generating sensors and two control sensors. One NO-generating sensor and one control sensor were placed in the carotid arteries, while the second pair was placed in the femoral arteries via 16-gauge Angiocath 1.16 inch cannulae. The cannula tips were trimmed off by ~ 1 cm to make an angle that allows for the ease of intravascular implantation. Sensors were slid into the cannulae and fixed to the 4-way stopcock by epoxy. Approximately a 1 cm length of the sensing catheter extended past the end of the cannula and was exposed to flowing blood in the animal. The artery distal to the cannula insertion was not ligated. Slow saline drips (0.1–0.2 mL/min) containing 1 U/mL of heparin were supplied to each sensor site via pressure bags to prevent back-flow of blood into the cannulae. Sensors were implanted such that the sensor tip was exposed to oncoming blood flow and the small amount of heparin present in the saline drips was washed distally from the sensor, never flowing over the sensor surface.

No systemic anticoagulation agent was administered during each animal study. Activated coagulation times (ACT) were measured before sensor implantation and was checked every 4 h during the experiment to ensure that the slow heparin infusion does not lead to any significant systemic anticoagulation. One hour after implantation, sensors were calibrated *in situ* via a one point calibration (assuming zero current for zero oxygen level and that the observed current corresponds to the blood oxygen PO_2 level measured *in vitro* by the ABL-505 blood gas monitor at the point of calibration). Continuous amperometric sensor output was recorded, and discrete blood samples were drawn periodically and analyzed by the ABL-505 to evaluate the accuracy of the implanted sensors' performance. During the first 2 h, blood samples were drawn every 15 min, and during hours 3–4, samples were drawn every 30 min. During the remainder of the experiment, samples were drawn every hour for comparison purposes. In total, 24 oxygen sensing catheters were evaluated (12 NO-generating sensors and 12 controls) in the 3- μ m particle group and a total of 12 (6 NO-generating and 6 controls) were studied in the nanoparticle group.

Upon termination of every animal preparation, the femoral and carotid arteries were excised distal to the implanted sensor. The animal was then euthanized with a bolus injection of Fatal-Plus (Vortech Pharmaceutical, Dearborn, MI). To prevent scraping off of the surface bio-layer, the sensors were carefully dissected from the arteries without pulling them out of the vessels or through the cannula, and rinsed in PBS to remove loosely adsorbed blood elements.

2.6. Surface clot evaluation

Digital images of the oxygen sensing catheters were taken immediately after the removal of sensors from the blood vessels. A lactate dehydrogenase (LDH) assay has been reported previously as a useful approach for quantifying platelet adhesion to surfaces [29]. In this paper, this LDH assay was used to assess the degree of gross thrombus and cell adhesion on the sensor surfaces after the *in vivo* experiments. The portion of catheter tips that had been exposed to the blood stream was cut off and stored in 1.5 mL lysis buffer solution (PBS buffer with 1 wt% Triton X-100 and 0.75 wt% bovine serum albumin) for 1 h to lyse any cells that were adhered on the catheter surfaces. The copper-loaded catheter tips were then saved and later tested for the NO generation *in vitro* to assess whether exposure to flowing blood significantly changes the ability to catalyze the RSNO decomposition. The lysate solution was then further diluted 1:5 with the lysing buffer. One hundred μ L of the final lysate was mixed, in triplicate samples, with 100 μ L of reagent from an LDH assay kit (Roche Applied Sciences, Indianapolis, IN) into wells of a 96-well polystyrene microplate (Fisher) and the absorbance at 490 nm was

monitored by a Labsystems Multiskan RC microplate reader (Fisher). The linear portion of absorbance vs. time curve was used for quantitating LDH activity.

3. Results and Discussion

3.1. NO-generating polymer coatings

In preliminary experiments, a variety of polymer matrices containing 3- μm Cu^0 particles were tested, among which the 2:1 blend of RTV-3140 silicone rubber and Tecophilic SP-60D-60 HPPU yielded the optimal balance of adhesiveness to the SR tubing of the catheter and adequate hydrophilicity to allow diffusion of RSNO species into the polymeric layer containing the Cu^0 particles. The optimal particle:polymer ratio (40 w/w% for 3- μm and 33 w/w% for 80-nm particles) was determined by the peak fluxes of NO generation from GSNO for each formulation. Another goal was to use the least possible amount of copper so as to minimize any potential toxic effects [30] that may be caused by continuous copper corrosion. Previous *in vivo* experiments [17,19] that employed NO-releasing polymer films required thick polymer coatings (~ 100 μm) in order to achieve the desired flux and duration of NO release. Since the NO-generation strategy suggested here only requires a very thin layer of Cu^0 catalyst to be immobilized at the sensor surface, the thickness of the sensor coating with 3- μm particles could be reduced to as little as ~ 7 μm , while coatings can be even thinner for films containing the Cu^0 nanoparticles. At the same time, using the 3- μm Cu^0 particles produces slightly rougher sensor surfaces than the controls (based on scanning electron micrographs (SEM), not shown here). This may put the NO-generating sensors at a disadvantage since rougher surfaces are prone to induce more thrombus formation [31]. However, it was found that much smoother surfaces can be readily achieved using the polymer films containing the Cu^0 nanoparticles as the catalytic layer, with negligible change of surface roughness as determined by SEM. The utilization of an adhesion promoter layer allows for the use of polyurethanes as the coating material to load the copper nanoparticles on the silicone rubber surfaces of the catheters. Tecoflex SG-80A was found to offer the best combination of NO flux and adhesive properties in this case.

In preliminary *in vitro* experiments to assess NO generation capability of the different coatings, the GSNO and GSH concentrations were set at 1 μM and 30 μM , respectively, which is close to their physiological levels [23]. As shown in Fig. 2, the NO-generating polymer coatings on sensor sleeves, either made from 3- μm (Fig. 2-1) or 80-nm Cu^0 particles (Fig. 2-2), were capable of generating physiologically relevant ($>1 \times 10^{-10}$ $\text{mol cm}^{-2} \text{min}^{-1}$) levels of NO both before and after implantation within a porcine artery for 20 h. The levels of generated NO detected by chemiluminescence decrease over time as the GSNO substrate in the test solution is consumed. The sensor sleeves tested were different in length before (25 mm) and after (10 mm) the *in vivo* study, as only the exposed portion was taken after the implantation. Thus, the NO flux data were normalized to reflect this change in surface area. Interestingly, the sensors coated with polymer containing the 3- μm Cu^0 particles actually generated higher fluxes after the *in vivo* experiment. This might be due to the hydrophilic moiety in the polymer becoming more completely hydrated allowing for faster GSNO diffusion into the film. Although there is no method currently available to directly measure the NO fluxes at the sensor surfaces *in vivo*, it is anticipated that the oxygen sensors coated with the films containing the Cu^0 particles are, in fact, able to continuously generate NO *in vivo* from endogenous RSNO substrates.

Our previous results with NO-releasing polymers showed that NO released from the sensor surface does not interfere with its oxygen measurements during the time frame of the *in vivo* experiments [17]. In this study, the possible effects of adding the copper particles to the outer layer of the sensor on the amperometric oxygen sensitivity and response times of the devices was also examined. Fig. 3 illustrates the typical current responses to different levels of PO_2 displayed by the NO-generating sensors based on the 3- μm and nano- Cu^0 particles embedded

in the outer polymer coatings. As shown, the introduction of the Cu⁰ catalysts does not significantly impact the electrochemical oxygen response of the sensors, with responses linear to at least 227 mmHg (30% O₂ balanced by N₂) and no dramatic change in response time (compared to control sensors without the coatings). As shown in Fig. 3, the output currents of given sensors do vary as the result of different working electrode areas exposed in the fabrication step. This is the reason why *in vivo* calibration needs to be performed at the beginning of each experiment.

3.2. In vitro copper corrosion

Since it is known that the catalytic species required to decompose RSNO species to NO is either Cu(I) or Cu(II) ions, the NO generation process observed must be due to a slow corrosion of the metallic copper particles in the polymeric matrix. Further, copper is an essential trace element in the biological systems. The average intake of copper by human adults ranges from 0.6 – 1.6 mg/d [32]. While trace amounts of copper are vital for the healthy functioning of organisms, excess copper build-up in the body could cause Wilson's disease which may lead to impaired liver function [30]. Given that NO-generation of the outer polymeric layers of the oxygen sensing catheters relies on the corrosion of metallic copper particles to provide reactive surface ions, it is critical to establish that copper corrosion is well below the level required for safe use under physiological conditions. Copper analysis via the colorimetric BCA assay has excellent sensitivity and selectivity, and the results have been reported to correlate very well with a conventional atomic absorption method [28]. Using this assay, the levels of copper ions present in PBS solutions in which a Cu⁰ particle based coatings were soaked in for at least 24 h were measured. The corrosion rate for copper was determined to be 4.84 ± 0.37 μg/d (N = 4) per catheter sleeve for coatings that contain the 3-μm Cu⁰ particles and 0.78 ± 0.17 μg/d (N = 3) for the Cu⁰ nanoparticle-based coating. In both cases, this is less than 1% of the recommended daily intake for human adults [32]. Therefore, with only 4 relatively small sensors implanted in each animal, it is unlikely that copper leaching from the surface of the sensors will have any toxic effects. Moreover, the sensors were implanted in a dynamic flow environment so that there would not be any locally accumulated copper levels to be concerned about. In fact, no unusual inflammation was observed at any of the sensor implant sites that were used to carry out the animal experiments reported in this study.

3.3. Blood-compatibility and surface thrombus evaluation

3.3.1. 3-μm Cu⁰ particle coated sensors—Without administration of a systemic anticoagulation agent, 12 pairs of control and NO-generating sensors were implanted in porcine carotid and femoral arteries for at least 20 h. The animals' ACTs remained within the normal range of 75–120 s throughout, suggesting no systemic effects of the heparin drips at each sensor site. Any gross thrombi on the surfaces of the implanted sensors were determined by observing formation of mature blood clot with a dark color and fibrin networks after the sensors were excised from the arteries. For all the oxygen sensors implanted, 9 of 12 control sensors showed visible thrombus formation after being explanted and rinsed in PBS; in contrast, only 3 of 12 NO generating sensors had visible clots on them. In all cases where one or two NO-generating sensors developed observable blood clots, both control sensors in the same animal had significant clots over them as well. This might imply that lower than normal RSNO levels existed in these test animals. In such cases the NO-generating functionality of the Cu⁰ particle coatings would not provide adequate surface levels of NO to improve thromboresistance.

Two representative pairs of sensors in the 3-μm Cu⁰ particle group after explantation are shown in Fig. 4-1 and Fig. 4-2, each pair from the same animal. In each panel (A) represents NO-generating sensors and (B) represents the control sensors. To the right of the dashed lines is the portion of the sensors that have been exposed to blood flow. In general, NO-generating sensors are darker in color than the controls due to the copper particles in the outer polymeric

coating. Both NO-generating sensors (i.e., A1 and A2) appear clean. However, a mature blood clot has developed over control sensor B1. Control sensor B2 appears to be free of clot. Only 3 of 12 control sensors exhibited such thrombus-free surfaces after being explanted.

SEM is normally used for the surface analysis of blood-contacting materials [33]. It is ideal in providing detailed image at a very small region of the surface but fails to give quantitative information on a macroscopic scale. In this study, an LDH assay was used to better quantify platelet and other cell adhesion to surfaces of the implanted oxygen sensing catheters. LDH is a very important metabolic enzyme commonly found in blood cells and an LDH assay has already been used determining the degree of platelet adhesion to surfaces *in vitro* [29,34,35]. The LDH content of a given cell is normally proportional to its size [29]. Table 1 lists the corresponding LDH assay results of the two specific pairs of sensors examined above. Not surprisingly, sensor B1 exhibited substantial LDH activity in the resulting lysate solution (37.4 mU) whereas sensor A1 showed significantly less LDH activity. Overall, a summary of LDH assay data for all 3- μm Cu^0 particle coated sensors (N=12) and their corresponding controls is provided in Table 1. As can be seen, the average amount of LDH activity on control sensors is nearly 10 fold the levels found on the sensors fabricated with the polymer coating containing the 3- μm copper particles. These two data sets are statistically different at the 95% confidence interval ($p = 0.022$ with 22 degrees of freedom).

3.3.2. Cu^0 nanoparticle coated sensors—Coatings with Cu^0 nanoparticles yielded similar results as those with 3- μm Cu^0 particles. Overall, three out of six control sensors developed mature blood clots on the surface while only one NO-generating sensor had surface clot. Figs. 4-3 and 4-4 also show two typical pairs of nanoparticle coated sensors. Sensors A3 and A4, the two NO-generating devices, both turned out to be relatively clean after 19 h of implantation. Control sensor B4 was also blood clot free. However, a mature clot that developed around control sensor B3 had completely engulfed the sensing tip. The LDH assay results for these two pairs of sensors, as well as the statistical analysis of the entire Cu^0 nanoparticle test group (N=6), are summarized in Table 1. Again, on average, the sensors coated with the polymer film containing the Cu^0 nanoparticles tend to have much lower LDH activity originating from their surfaces, suggesting that much less cell adhesion occurs for this group. The difference in LDH activities between NO-generating and control sensors in this category is also statistically significant ($p = 0.013$). The LDH assay results are not affected by the small amount of corroded copper that is present in the lysate solution. A control experiment with free LDH in the presence and absence of 1 $\mu\text{g}/\text{mL}$ Cu^{2+} ions (much higher than the possible amount of leached copper during the 1 h incubation period, see 3.2) showed the same LDH enzyme activities.

3.4. In vivo O_2 sensor performance

3.4.1. 3- μm Cu^0 particle coated sensors—The corresponding PO_2 levels determined by the two pairs of sensors from Figs. 4-1 and 4-2, as well as the ‘true values’ obtained from *in vitro* blood gas analyzers measurements over 20 h of implantation, are shown in Figs. 5-1 and 5-2. Implanted sensors are able to track closely with the PO_2 values measured by benchtop blood gas analyzer when their surfaces are not covered by blood clots, as were the case for both NO-generating sensors in Fig. 5-1 and 5-2, and the control sensor in Fig. 5-2 (sensor B2). However, when blood clots developed over the sensor surfaces, the metabolism of cells with the clot consumes oxygen, rendering false- negative in the PO_2 measured by such sensors. The extent of surface clot dictates the deviation from true values. As seen in Fig. 5-1, sensor B1, which had a complete coverage of clot over the sensing tip, started to show false- negative oxygen values 5 h into the experiment and eventually provided readings that were $\sim 20\%$ of the true PO_2 values. On the other hand, control sensor B2 in Fig. 5-2, and both NO-generating sensors (A1 and A2) in Figs. 5-1 and 5-2, which had clean surfaces, traced PO_2 levels quite

accurately. Such variations in the analytical performance of control sensors reflect the biocompatibility issues usually encountered with intravascular sensors, with some sensors completely covered by blood clot while others remain relatively clean.

Fig. 6-1 summarizes the *in vivo* analytical results for both NO-generating and control sensors (N = 12 each) in the 3- μm copper particle coated group. The average percent deviations (from the true values derived from benchtop blood gas machine) of O_2 levels determined by each set of implanted sensors, as well as their standard deviations, are plotted as a function of time. It is clear that the NO-generating sensors yield more accurate PO_2 results overall, with the percentage deviation ranging only from -12% to +9% and the average values of PO_2 nicely straddling the true values throughout the experiment. The control sensors, however, consistently exhibited negative deviations greater than -20% from the 6 h point forward, with the largest average error being -42% at the 12 h time point. Such lowered responses to O_2 correlated very well with the observed surface thrombosis on these control sensors. The standard deviations of the control set were also significantly larger than those in the NO-generating set. Table 2 lists the average percent deviation of NO-generating and control sensors at 5, 10, 15 and 20 h time points as well as their 95% confidence intervals. The difference between the measurements made by NO-generating sensors and that derived from benchtop blood gas machine (considered 100% accurate) was not statistically significant at any time point during the experiment. In contrast, the control sensors showed statistically significant differences (at 95% confidence) at 15 and 20 h time points when compared to *in vitro* blood gas results. Indeed, the control sensor results were statistically different from blood gas values from 11 h onwards. Moreover, the PO_2 values measured by control sensors were statistically different from that measured via NO-generating sensor at 95% confidence level ($t = 2.31$, $p = 0.031$ with 22 degrees of freedom) at the final 20 h time point.

3.4.2. Cu^0 nanoparticle coated sensors— PO_2 values recorded from the same two pairs of Cu^0 nanoparticle coated sensors shown in Fig. 4-3 and 4-4 are illustrated in Figs. 5-3 and 5-4. The results are quite similar to that observed with the 3- μm Cu^0 particle coatings. Sensors with little or no blood clots (i.e., sensors A3, A4 and B4) traced well with corresponding *in vitro* blood gas measurements. In contrast, sensor B3, a control sensor, which was completely covered by clot, yielded significantly lower PO_2 values from the 5 h point forward and actually reported values of oxygen that were near zero.

Fig. 6-2 provides a summary of the *in vivo* oxygen sensing data obtained from the six pairs of sensors coated with the copper nanoparticle layer. Again, NO-generation via the presence of the Cu^0 nanoparticle catalyst provides more accurate *in vivo* measurements of PO_2 throughout the 19 h implantation period. The average percent deviation from *in vitro* blood gas readings ranged from -11% to +12%. Control sensors show considerable (>20%) false negatives after 5 h into the experiment, with average PO_2 values deviating up to -36% at 10 h. Like the control group of 3- μm Cu^0 particles, greater standard deviations were also observed in the nanoparticle control sensor group. The average percent deviation at 5, 10, 15 h and the 95% confidence interval of measurements derived from each group are listed in Table 3. Statistical analysis of the data shown in Table 3 for the nanoparticle coated sensors indicates that the NO-generating sensors accurately traced PO_2 levels at the 95% confidence interval level (no statistically significant deviations from *in vitro* values), but the control sensor measurements did not agree with the true values at the same confidence interval from the 10 h point forward.

4. Conclusion

Copper particle-based polymer coatings capable of generating physiological levels of NO in the presence of endogenous RSNO species have been applied to the surface of intravascular electrochemical oxygen sensing catheters. These sensors, when tested *in vivo* via a porcine

artery model, exhibit improved blood-compatibility over the control sensors as evidenced by less propensity toward surface thrombus formation and more accurate analytical results. Three out of 12 NO-generating sensors in the 3- μ m particle group, and 1 out of 6 NO-generating sensors in the nanoparticle group showed some degree of blood clot on the surfaces. This might be the result of low RSNO levels in these animals and hence NO levels generated were not sufficient to completely suppress thrombus formation. It should also be noted that the surface of NO-generating sensors were not as smooth as that of the control sensors, especially for the larger copper particles, which is disadvantageous in terms of preventing clot formation. However, there is still a statistical difference between the two groups of sensors. At 95% confidence level, the NO-generating sensors agreed very well with *in vitro* blood gas measurements with no statistically significant differences throughout the experiment. On the other hand, control sensors results were statistically different from *in vitro* blood gas measurements after about 10 h implantation.

The control sensor behavior found in this work is representative of intravascular sensing devices developed thus far, which explains their limited use in real clinical applications. The NO-generation strategy offers a potential solution to this problem and may find use in other blood-contacting devices as well. Ongoing research in this group is focusing on covalently linking various species to polymers that can provide the same NO-generation capability as the copper particles used here. New polymers containing immobilized organoselenium species [36] appear most promising as new NO generating materials for such implantable sensor applications.

Acknowledgements

The authors would like to thank the National Institutes of Health for funding this research work (Grant #: EB-000783 and EB-004527).

References

1. Frost MC, Meyerhoff ME. Implantable chemical sensors for real-time clinical monitoring: progress and challenges. *Curr Opin Chem Biol* 2002;6:633–641. [PubMed: 12413548]
2. Mahutte CK. On-Line Arterial Blood Gas Analysis With Optodes: Current Status. *Clin Biochem* 1998;31:119–130. [PubMed: 9629484]
3. Meyerhoff ME. In-Vivo Blood-Gas and Electrolyte Sensors - Progress and Challenges. *Trends Anal Chem* 1993;12:257–266.
4. Fogt E. Continuous ex vivo and in vivo monitoring with chemical sensors. *Clin Chem* 1990;36:1573–1580. [PubMed: 2201462]
5. Andrade JD, Hlady V. Protein Adsorption and Materials Biocompatibility - a Tutorial Review and Suggested Hypotheses. *Adv Polym Sci* 1986;79:1–63.
6. Horbett, TA.; Ratner, BD.; Hoffman, AS.; Schoen, FJ.; Lemons, JE., editors. *Biomaterials Science - An Introduction to Materials in Medicine*. 2. Elsevier Academic Press; San Diego, CA: 2004. p. 237-246.
7. Hanson, SR.; Ratner, BD.; Hoffman, AS.; Schoen, FJ.; Lemons, JE., editors. *Biomaterials Science - An Introduction to Materials in Medicine*. 2. Elsevier Academic Press; San Diego, CA: 2004. p. 332-338.
8. Lisman T, Weeterings C, de Groot PG. Platelet aggregation: Involvement of thrombin and fibrin(ogen). *Front Biosci* 2005;10:2504–2517. [PubMed: 15970513]
9. Heemskerk JWM, Bevers EM, Lindhout T. Platelet activation and blood coagulation. *Thromb Haemost* 2002;88:186–193. [PubMed: 12195687]
10. Diodati JG, Quyyumi AA, Hussain N, Keefer LK. Complexes of Nitric-Oxide with Nucleophiles as Agents for the Controlled Biological Release of Nitric-Oxide - Antiplatelet Effect. *Thromb Haemost* 1993;70:654–658. [PubMed: 8115991]

11. Ignarro LJ, Buga GM, Wood KS, Byrns RE, Chaudhuri G. Endothelium-Derived Relaxing Factor Produced and Released from Artery and Vein is Nitric Oxide. *Proc Natl Acad Sci USA* 1987;84:9265–9269. [PubMed: 2827174]
12. Radomski M, Palmer R, Moncada S. An L-Arginine/Nitric Oxide Pathway Present in Human Platelets Regulates Aggregation. *Proc Natl Acad Sci USA* 1990;87:5193–5197. [PubMed: 1695013]
13. Feldman PL, Griffith OW, Stuehr DJ. The Surprising Life of Nitric-Oxide. *Chem Eng News* 1993;71:26–38.
14. Radomski MW, Vallance P, Whitley G, Foxwell N, Moncada S. Platelet-Adhesion to Human Vascular Endothelium Is Modulated by Constitutive and Cytokine-Induced Nitric-Oxide. *Cardiovasc Res* 1993;27:1380–1382. [PubMed: 7504587]
15. Michiels C. Endothelial cell functions. *J Cell Physiol* 2003;196:430–443. [PubMed: 12891700]
16. Vaughn MW, Kuo L, Liao JC. Estimation of nitric oxide production and reaction rates in tissue by use of a mathematical model. *Am J Physiol (Heart Circ Physiol)* 1998;43:H2163–H2176.
17. Schoenfisch MH, Mowery KA, Rader MV, Baliga N, Wahr JA, Meyerhoff ME. Improving the thromboresistivity of chemical sensors via nitric oxide release: Fabrication and in vivo evaluation of NO-releasing oxygen-sensing catheters. *Anal Chem* 2000;72:1119–1126. [PubMed: 10740848]
18. Zhang HP, Annich GM, Miskulin J, Osterholzer K, Merz SI, Bartlett RH, Meyerhoff ME. Nitric oxide releasing silicone rubbers with improved blood compatibility: preparation, characterization, and in vivo evaluation. *Biomaterials* 2002;23:1485–1494. [PubMed: 11829445]
19. Frost MC, Rudich SM, Zhang HP, Maraschio MA, Meyerhoff ME. In vivo biocompatibility and analytical performance of intravascular amperometric oxygen sensors prepared with improved nitric oxide-releasing silicone rubber coating. *Anal Chem* 2002;74:5942–5947. [PubMed: 12498188]
20. Wong K, Li XB. Nitric oxide infusion alleviates cellular activation during preparation, leukofiltration and storage of platelets. *Transfus Apheresis Sci* 2004;30:29–39.
21. Wallis JP. Nitric oxide and blood: a review. *Transfus Med* 2005;15:1–11. [PubMed: 15713123]
22. Stamler JS, Jaraki O, Osborne J, Simon DI, Keaney J, Vita J, Singel D, Valeri CR, Loscalzo J. Nitric Oxide Circulates in Mammalian Plasma Primarily as an S-Nitroso Adduct of Serum-Albumin. *Proc Natl Acad Sci USA* 1992;89:7674–7677. [PubMed: 1502182]
23. Giustarini D, Milzani A, Colombo R, Dalle-Donne I, Rossi R. Nitric oxide and S-nitrosothiols in human blood. *Clinica Chimica Acta* 2003;330:85–98.
24. Jourdeheuil D, Hallen K, Feelisch M, Grisham MB. Dynamic state of S-nitrosothiols in human plasma and whole blood. *Free Radic Biol Med* 2000;28:409–417. [PubMed: 10699753]
25. Williams DLH. The chemistry of S-nitrosothiols. *Acc Chem Res* 1999;32:869–876.
26. Oh BK, Meyerhoff ME. Spontaneous catalytic generation of nitric oxide from S-nitrosothiols at the surface of polymer films doped with lipophilic copper(II) complex. *J Am Chem Soc* 2003;125:9552–9553. [PubMed: 12903997]
27. Hwang S, Cha W, Meyerhoff ME. Polymethacrylates with a Covalently Linked Cu(II)-Cyclen Complex for the In Situ Generation of Nitric Oxide from Nitrosothiols in Blood. *Angew Chem* 2006;118:2811–2814.
28. Brenner AJ, Harris ED. A Quantitative Test for Copper Using Bicinchoninic Acid. *Anal Biochem* 1995;226:80–84. [PubMed: 7785783]
29. Tamada Y, Kulik EA, Ikada Y. Simple Method for Platelet Counting. *Biomaterials* 1995;16:259–261. [PubMed: 7749004]
30. Daniel KG, Harbach RH, Guida WC, Dou QP. Copper storage diseases: Menkes, Wilson's, and cancer. *Front Biosci* 2004;9:2652–2662. [PubMed: 15358588]
31. Clarotti G, Schue F, Sledz J, Aoumar AAB, Geckeler KE, Orsetti A, Paleirac G. Modification of the biocompatible and haemocompatible properties of polymer substrates by plasma-deposited fluorocarbon coatings. *Biomaterials* 1992;13:832–840. [PubMed: 1457676]
32. Tapiero H, Townsend DM, Tew KD. Trace elements in human physiology and pathology. *Copper Biomed Pharmacother* 2003;57:386–398.
33. White, JG.; Gibbins, JM.; Mahaut-Smith, MP., editors. *Methods in Molecular Biology (Platelets and Megakaryocytes)*. 272. Humana Press; Totowa, NJ: 2004. p. 47-63.

34. Tsai WB, Grunkemeier JM, Horbett TA. Human plasma fibrinogen adsorption and platelet adhesion to polystyrene. *J Biomed Mater Res* 1999;44:130–139. [PubMed: 10397913]
35. Suggs LJ, West JL, Mikos AG. Platelet adhesion on a bioresorbable poly(propylene fumarate-co-ethylene glycol) copolymer. *Biomaterials* 1999;20:683–690. [PubMed: 10208411]
36. Cha W, Meyerhoff ME. Catalytic Generation of Nitric Oxide from S-Nitrosothiols Using Immobilized Organoselenium Species. *Biomaterials*. 2006Submitted for publication

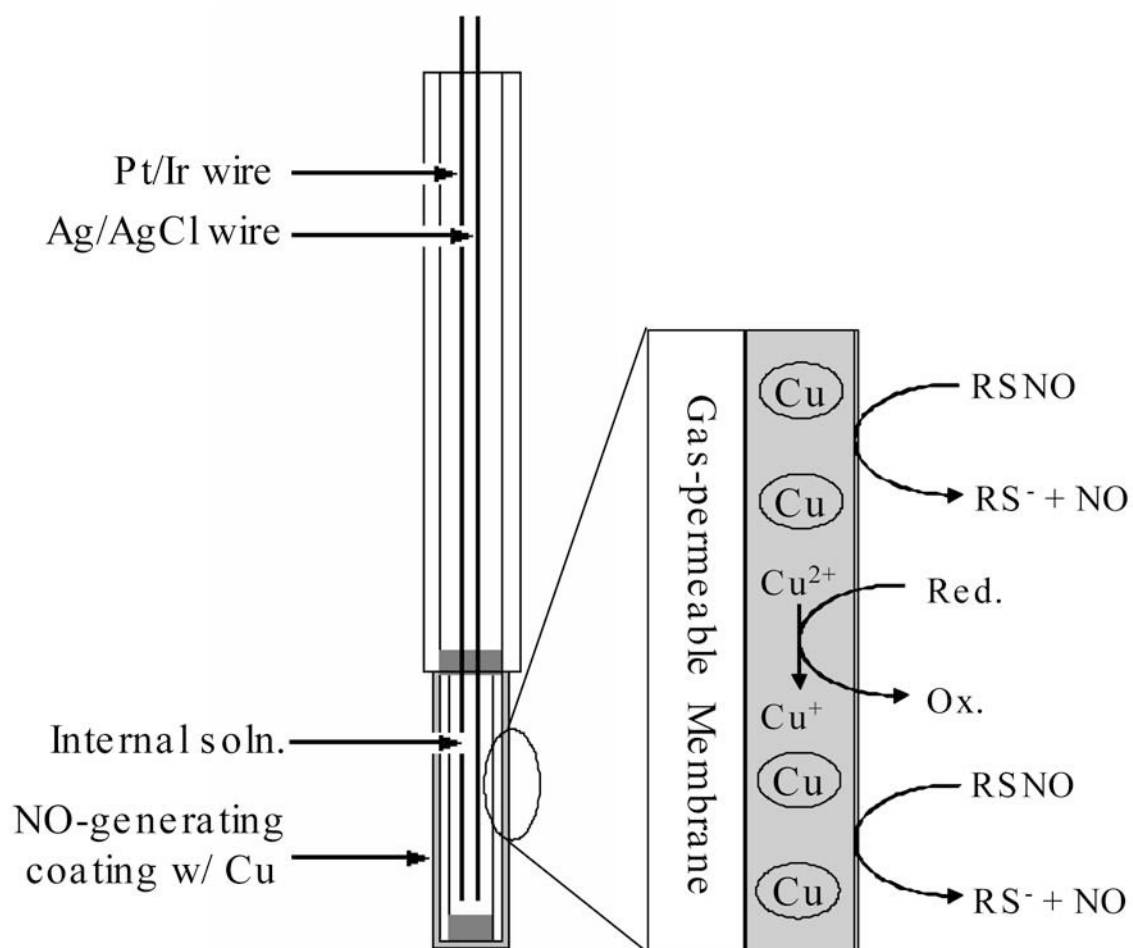


Figure 1. Schematic of intravascular oxygen sensor design and the NO generation mechanism.

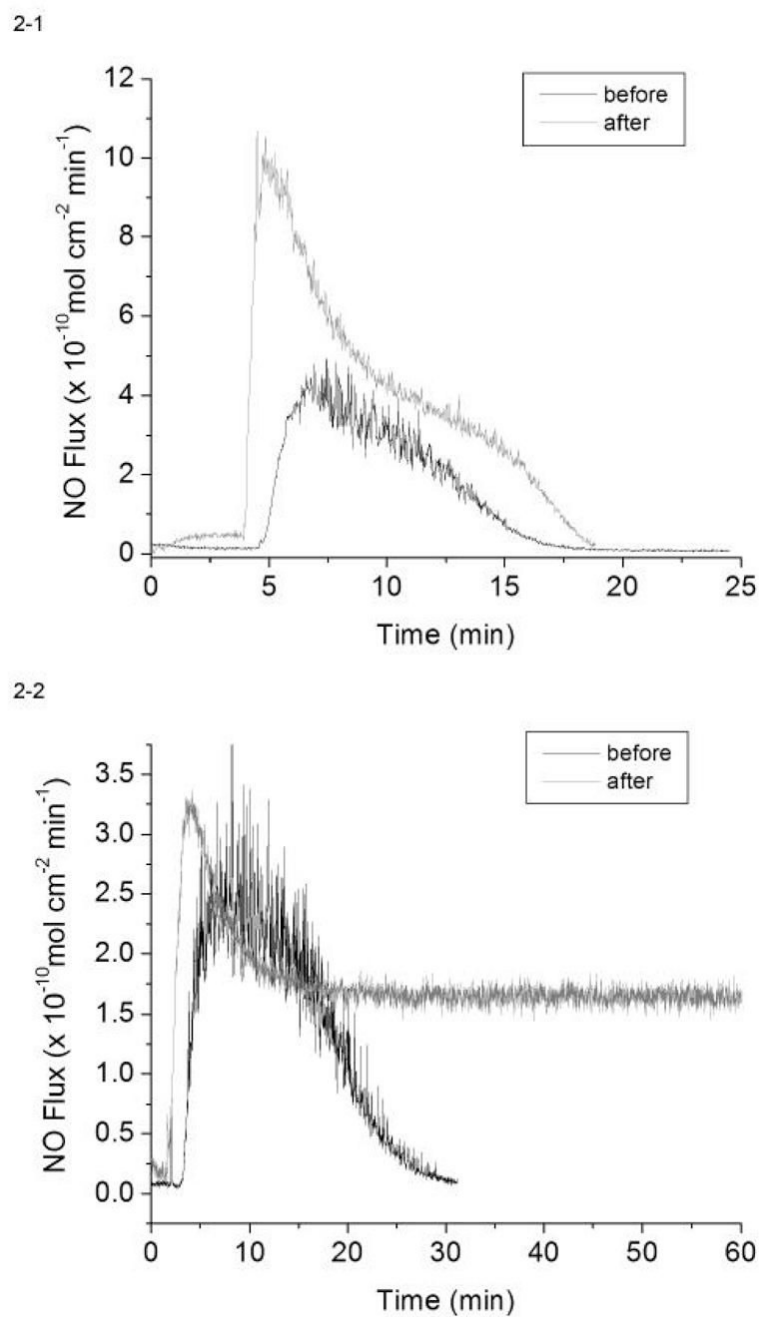


Figure 2.

In vitro generation of NO from 1 μM GSNO, 30 μM GSH and 5 μM EDTA in 2 mL PBS at 37°C by the catalysis of (1) 3 μm and (2) 80 nm Cu^0 particle coated sensor sleeves before and after animal studies.

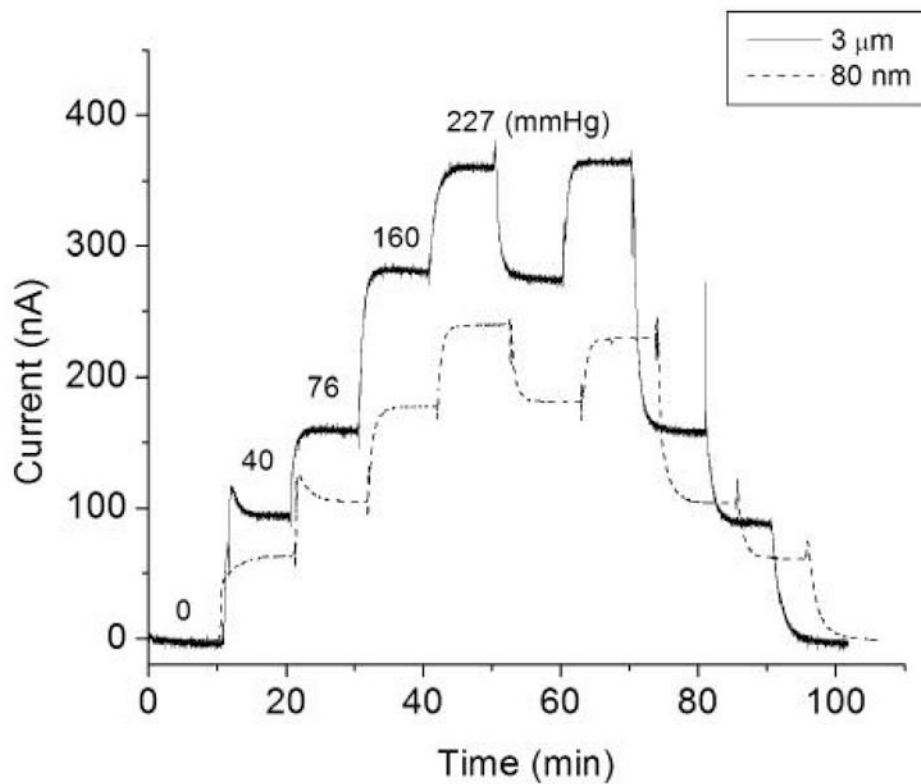
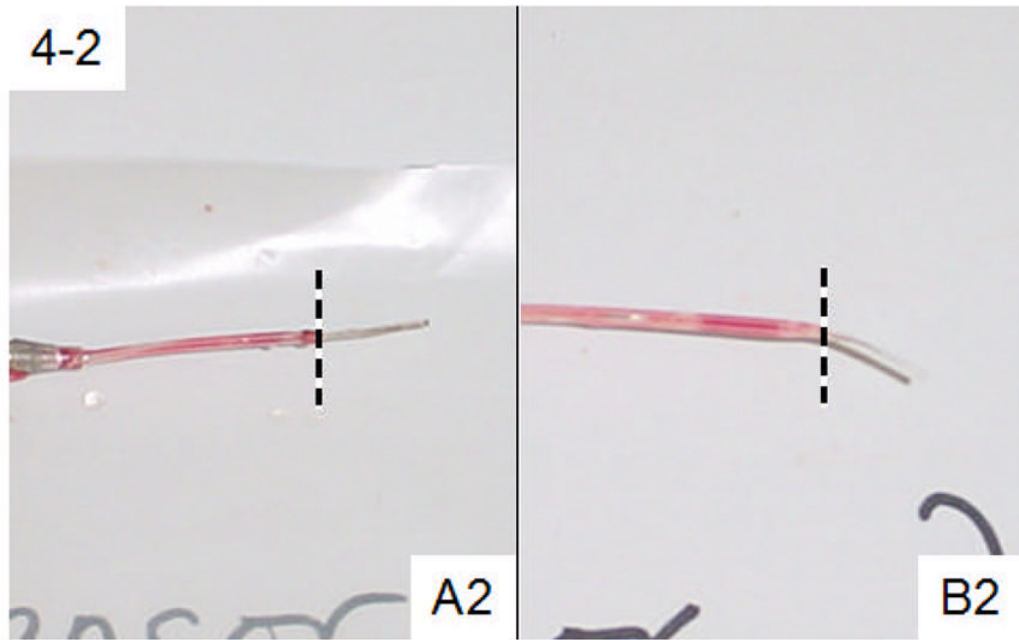
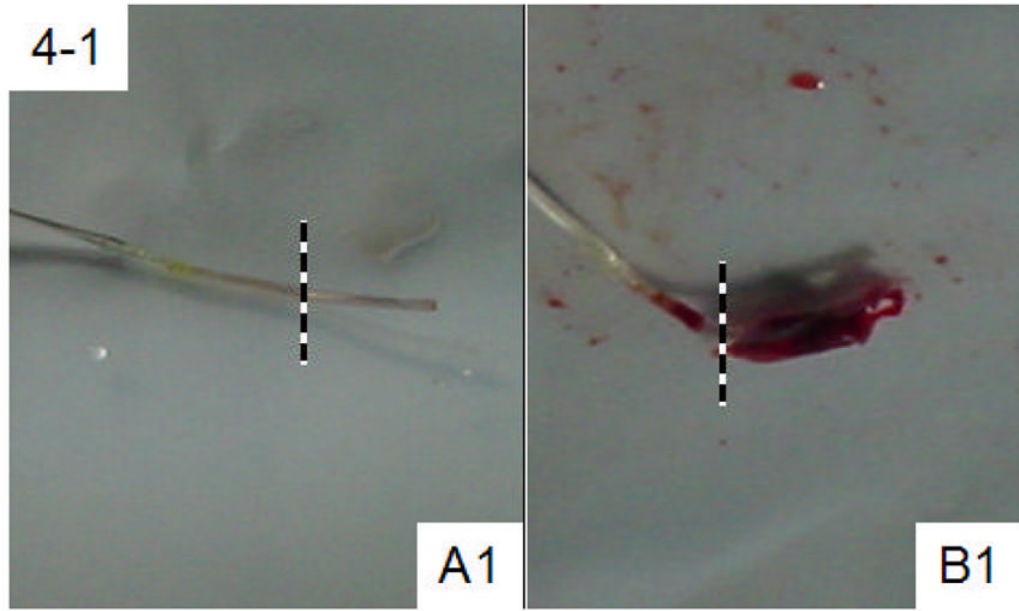


Figure 3. Amperometric responses of NO-generating oxygen sensors to 0, 5, 10, 21 and 30% oxygen balanced with nitrogen. The actual oxygen partial pressures are indicated for each oxygen level.



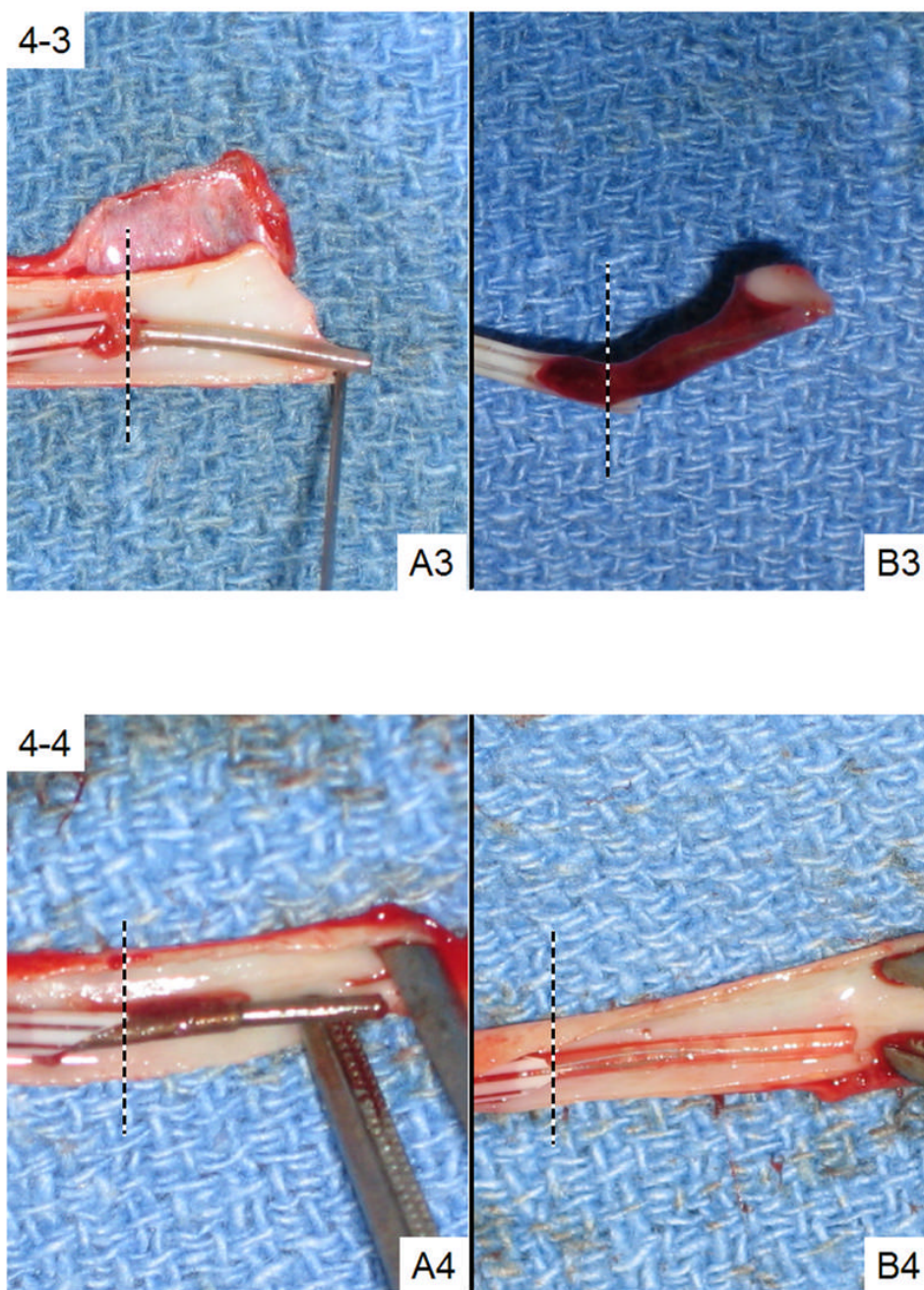
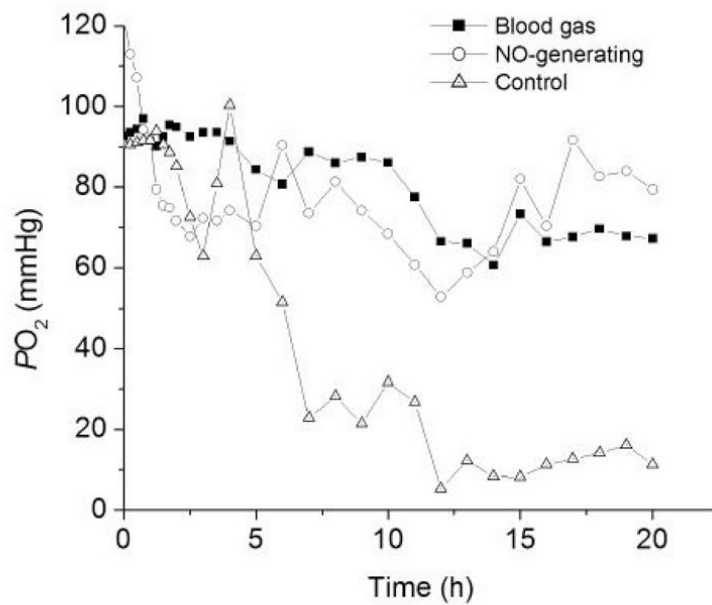
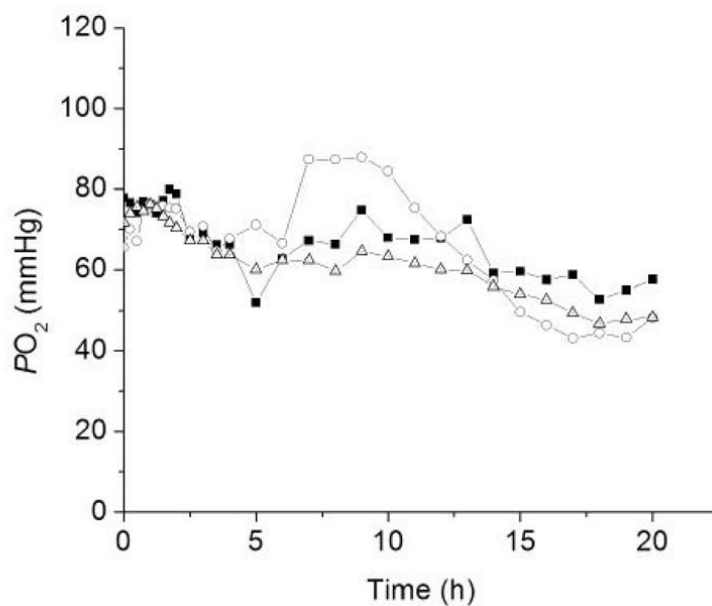


Figure 4. Images of four representative pairs of NO-generating (Panel A) and control (Panel B) sensors after *in vivo* studies. The portion to the right of the dotted lines had been exposed to blood. Sensors A1, B1, A2 and B2 are from the 3- μ m particle group while Sensors A3, B3, A4 and B4 are from nanoparticle group.

5-1



5-2



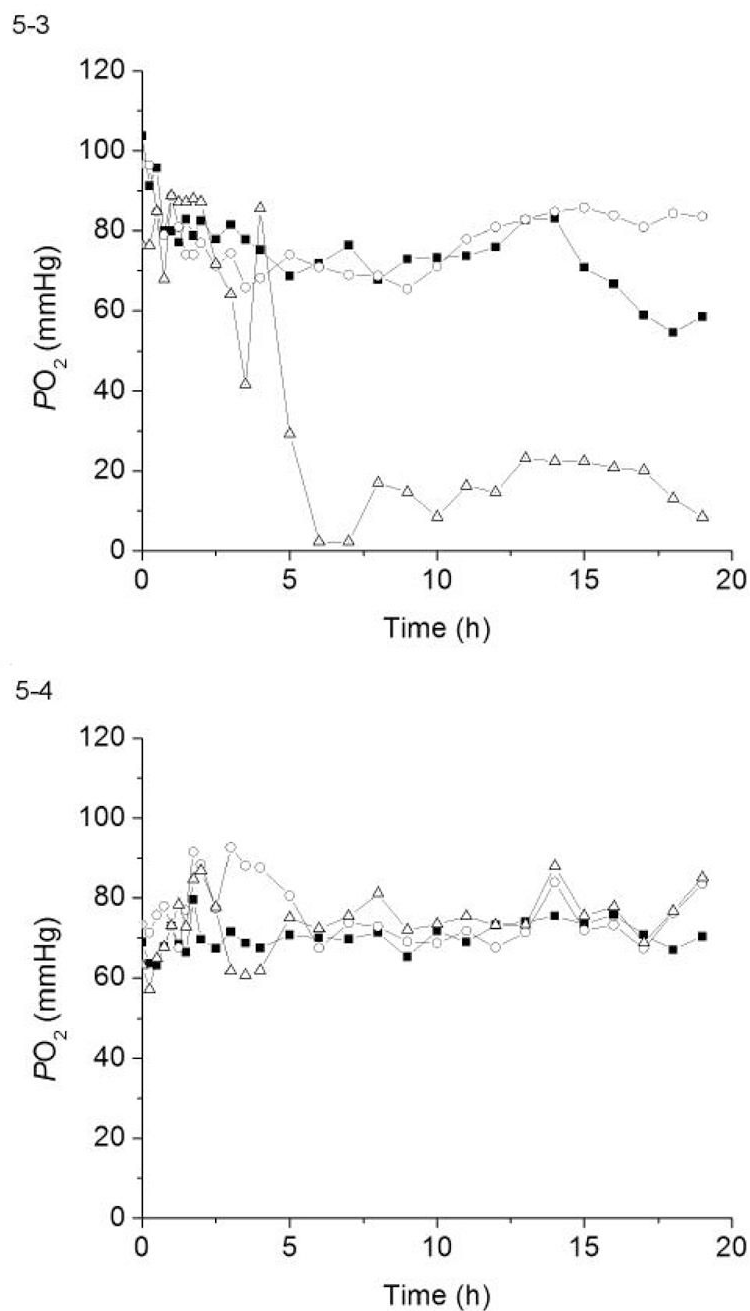


Figure 5. The PO_2 values measured by the same four pairs of NO-generating and control sensor shown in Fig. 4 as compared to the standard blood gas analyzer results for each experiment. (5-1) sensors A1 & B1; (5-2) sensors A2 & B2; (5-3) sensors A3 & B3, and (5-4) sensors A4 & B4.

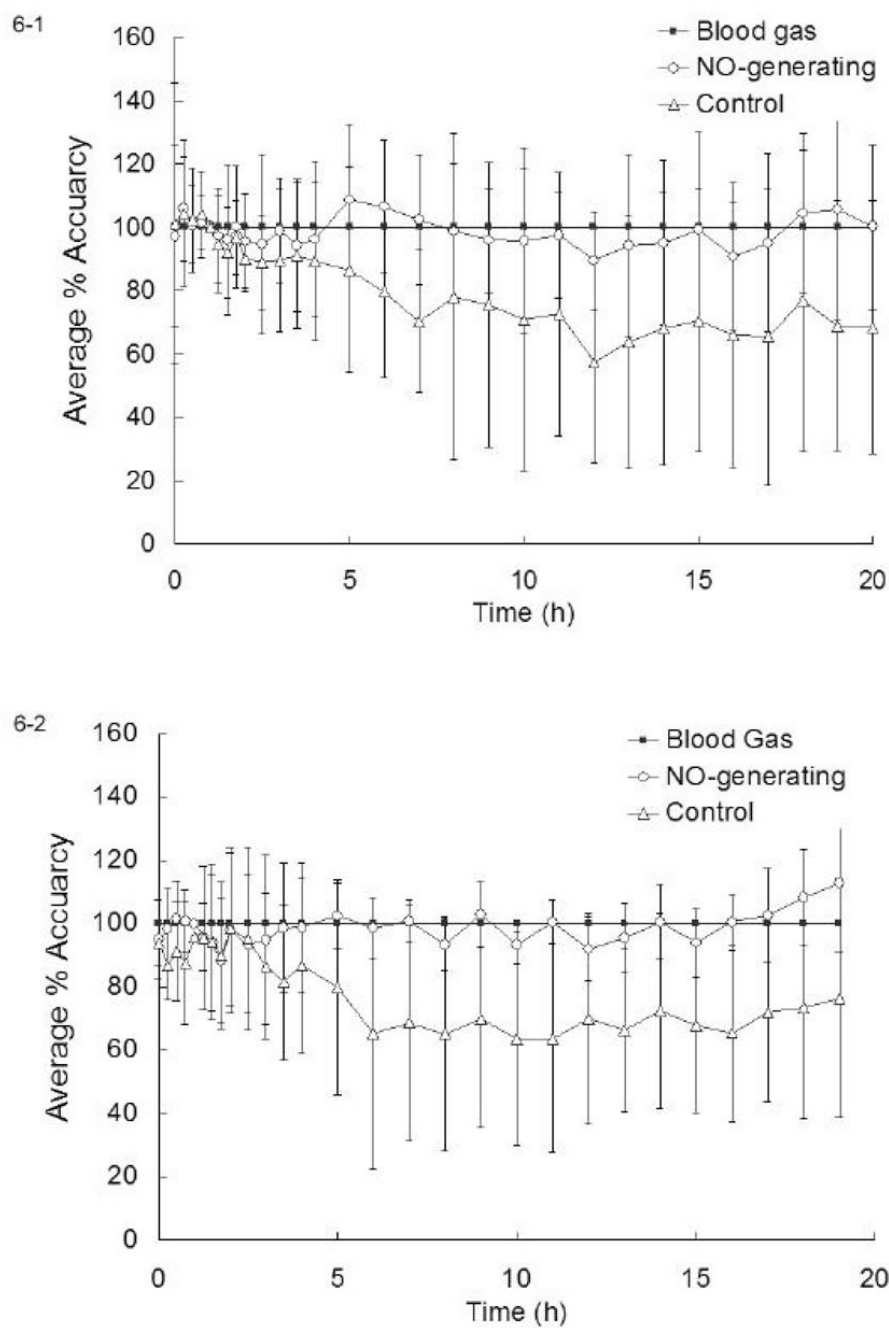


Figure 6. Plots of the average percent accuracy of: (1) NO-generating sensors based on 3- μm Cu^0 particles and control sensors (N = 12 each), and (2) NO-generating sensors based on 80 nm Cu^0 particles and control sensors (N = 6 each), as compared to *in vitro* blood gas analyzer results, which were considered 100% accurate.

Table 1

LDH assay of surface clots for the 4 pairs of sensors examined in Fig. 3, and the statistical results of LDH levels in the two groups.

Sensor Group	NO-generating (A)	Control (B)
A1 & B1	0.14	37.4
A2 & B2	1.67	0.11
3- μ m particle (N=12)	2.97 \pm 2.05	24.1 \pm 20.9
A3 & B3	5.18	38.8
A4 & B4	5.32	4.07
Nanoparticle (N=6)	3.22 \pm 2.54	25.3 \pm 22.2

Table 2

Average percent deviation and the 95% confidence intervals for PO_2 measurements made by sensors in the 3 μm particle group.

Time (h)	NO-generating sensors		Control sensors	
	Avg. % deviation	95% Conf. interval	Avg. % deviation	95% conf. interval
5	+ 8.6	\pm 15.1%	-13.6	\pm 20.6%
10	- 4.4	\pm 18.6%	-29.3	\pm 30.3%
15	- 0.8	\pm 19.5%	-29.6	\pm 26.4%
20	+ 0.2	\pm 16.6%	-31.7	\pm 25.4%

Table 3

Average percent deviation and the 95% confidence intervals for PO_2 measurements made by sensors in the nanoparticle group.

Time (h)	NO-generating sensors		Control sensors	
	Avg. % deviation	95% Conf. interval	Avg. % deviation	95% conf. interval
5	+ 2.4	± 10.9%	-20.2	± 35.6%
10	- 6.5	± 6.6%	-36.5	± 35.3%
15	- 6.1	± 11.4%	-32.2	± 28.8%